



University of  
Zurich<sup>UZH</sup>

Zurich Open Repository and  
Archive

University of Zurich  
University Library  
Strickhofstrasse 39  
CH-8057 Zurich  
[www.zora.uzh.ch](http://www.zora.uzh.ch)

---

Year: 2008

---

## Probing superconductivity in MgB2 confined to magnetic field tuned cylinders by means of critical fluctuations

Weyeneth, S ; Schneider, T ; Zhigadlo, N D ; Karpinski, J ; Keller, H

**Abstract:** We report and analyze reversible magnetization measurements on a high quality MgB2 single crystal in the vicinity of the zero-field transition temperature,  $T_c \simeq 38.83\text{K}$ , at several magnetic fields up to  $300\text{Oe}$ , applied along the  $c$ -axis. Although MgB2 is a two-gap superconductor our scaling analysis uncovers a remarkable consistency with 3D- $xy$  critical behavior, revealing that close to criticality the order parameter is a single complex scalar as in  $4\text{He}$ . This opens up the possibility that the superconducting transition in MgB2 is not a true phase transition. The order parameter cannot grow beyond the limiting magnetic length  $L_{Hi} = (0/(aH_i))^{1/2}$  with  $a \simeq 3.12$ , related to the averaged distance between the  $0/(a_j 0 k_0)$  and  $1/(T/T_c)^{4/3}$  with  $i \neq j \neq k$  and  $0, j_0, k_0$  denote the critical amplitudes of the correlation lengths above (+) and below (-)  $T_c$  superconductivity is confined to cylinders with diameter  $L_{Hi}(1D)$ . In contrast, above  $T_c$  and  $H_{pi}(T) = (0/(a_j 0 + k_0 +)) (T/T_c)^{4/3}$  the uncondensed pairs are confined to cylinders. Accordingly, there is no continuous phase transition in the plane along the  $H_{c2} -$  lines as predicted by the mean-field treatment.

DOI: <https://doi.org/10.1088/0953-8984/20/13/135208>

Posted at the Zurich Open Repository and Archive, University of Zurich

ZORA URL: <https://doi.org/10.5167/uzh-10513>

Journal Article

Accepted Version

Originally published at:

Weyeneth, S; Schneider, T; Zhigadlo, N D; Karpinski, J; Keller, H (2008). Probing superconductivity in MgB2 confined to magnetic field tuned cylinders by means of critical fluctuations. Journal of Physics: Condensed Matter, 20:135208.

DOI: <https://doi.org/10.1088/0953-8984/20/13/135208>

# Probing superconductivity in MgB<sub>2</sub> confined to magnetic field tuned cylinders by means of critical fluctuations

S Weyeneth<sup>1</sup>, T Schneider<sup>1</sup>, N D Zhigadlo<sup>2</sup>, J Karpinski<sup>2</sup>  
and H Keller<sup>1</sup>

<sup>1</sup> Physik-Institut der Universität Zürich, Winterthurerstrasse 190, CH-8057  
Zürich, Switzerland

<sup>2</sup> Laboratory for Solid State Physics, ETH Zürich, CH-8093 Zürich, Switzerland

E-mail: wstephen@physik.uzh.ch

**Abstract.** We report and analyze reversible magnetization measurements on a high quality MgB<sub>2</sub> single crystal in the vicinity of the zero field transition temperature,  $T_c \simeq 38.83$  K, at several magnetic fields up to 300 Oe, applied along the  $c$ -axis. Though MgB<sub>2</sub> is a two gap superconductor our scaling analysis uncovers remarkable consistency with 3D-xy critical behavior, revealing that close to criticality the order parameter is a single complex scalar as in <sup>4</sup>He. This opens up the window onto the exploration of the magnetic field induced finite size effect, whereupon the correlation length transverse to the applied magnetic field  $H_i$  applied along the  $i$ -axis cannot grow beyond the limiting magnetic length  $L_{H_i} = (\Phi_0 / (aH_i))^{1/2}$  with  $a \simeq 3.12$ , related to the average distance between vortex lines. We find unambiguous evidence for this finite size effect. It implies that in type II superconductors, such as MgB<sub>2</sub>, there is the 3D to 1D crossover line  $H_{pi}(T) = \left( \Phi_0 / \left( a\xi_{j0}^- \xi_{k0}^- \right) \right) (1 - T/T_c)^{4/3}$  with  $i \neq j \neq k$  and  $\xi_{i0,j0,k0}^\pm$  denotes the critical amplitudes of the correlation lengths above (+) and below (−)  $T_c$  along the respective axis. Consequently, above  $H_{pi}(T)$  and  $T < T_c$  superconductivity is confined to cylinders with diameter  $L_{H_i}(1D)$ . In contrast, above  $T_c$  and  $H_{pi}(T) = \left( \Phi_0 / \left( a\xi_{j0}^+ \xi_{k0}^+ \right) \right) (T/T_c - 1)^{4/3}$  the uncondensed pairs are confined to cylinders. Accordingly, there is no continuous phase transition in the  $(H, T)$ -plane along the  $H_{c2}$ -lines as predicted by the mean-field treatment.

PACS numbers: 74.25.Bt, 74.25.Ha, 74.40.+k

## 1. Introduction

Since the discovery of superconductivity in  $\text{MgB}_2$ [1] many important properties have already been measured, particularly outside the regime where thermal fluctuations dominate. The observation of thermal fluctuation effects have been limited in conventional low- $T_c$  superconductors because the large correlation volume makes these effects very small compared to the mean-field behavior. By contrast, the high transition temperature  $T_c$  and small correlation volume in a variety of cuprate superconductors lead to significant fluctuation effects[2, 3]. In  $\text{MgB}_2$  the correlation volume and  $T_c$  lie between these extremes, suggesting that fluctuation effects will be observable. Indeed, excess magnetoconductance[4], fluctuation effects in the specific heat[5], and fluctuating diamagnetic magnetization[6] was observed recently in powder samples. Here we report and analyze reversible magnetization data of a high quality  $\text{MgB}_2$  single crystal in the vicinity of the zero field transition temperature,  $T_c \simeq 38.83$  K, at several magnetic fields up to 300 Oe, applied along the  $c$ -axis. Though  $\text{MgB}_2$  is a two gap superconductor our scaling analysis uncovers below  $T_c$  remarkable consistency with 3D-xy critical behavior, revealing that the order parameter is a single complex scalar as in  $^4\text{He}$ . The high quality of the single crystal made it possible to enter this regime. For this reason the magnetic field induced finite size effect, whereupon the correlation length transverse to the applied magnetic field cannot grow beyond the limiting magnetic length  $L_{H_i} = (\Phi_0 / (aH_i))^{1/2}$ , with the magnetic field  $H_i$  applied along the  $i$ -axis and  $a \simeq 3.12$ , could be verified and studied in detail.  $L_{H_i}$  is related to the average distance between vortex lines. Indeed, as the magnetic field increases, the density of vortex lines becomes greater, but this cannot continue indefinitely, the limit is roughly set on the proximity of vortex lines by the overlapping of their cores. This finite size effect implies that in type II superconductors, superconductivity in a magnetic field is confined to cylinders with diameter  $L_{H_i}$ . Accordingly, there is below  $T_c$  the 3D to 1D crossover line  $H_{pi}(T) = (\Phi_0 / (a\xi_{j0}^-\xi_{k0}^-)) (1 - T/T_c)^{4/3}$  with  $i \neq j \neq k$ .  $\xi_{i0,j0,k0}^\pm$  denotes the critical amplitudes of the correlation lengths above (+) and below (-)  $T_c$  along the respective axis. It circumvents the occurrence of the continuous phase transition in the  $(H, T)$  -plane along the  $H_{c2}$ -lines predicted by the mean-field treatment. Furthermore, our analysis of the magnetization data of Lascialfari *et al.*[6] taken on a  $\text{MgB}_2$  powder sample also confirms that there is a magnetic field induced finite size effect above  $T_c$  as well. It leads to the line  $H_{pi}(T) = (\Phi_0 / (a\xi_{j0}^+\xi_{k0}^+)) (T/T_c - 1)^{4/3}$ , where the 3D to 1D crossover occurs and the uncondensed pairs are forced to confine in cylinders.

The paper is organized as follows: Next we sketch the scaling theory appropriate for a neutral type II superconductor with a single complex scalar order parameter falling in the absence of a magnetic field onto the 3D-xy universality class. Section II is devoted to experimental details, the presentation of our magnetization data for  $T \lesssim T_c$ , their analysis by means of the scaling theory and the analysis of the magnetization data of Lascialfari *et al.*[6] taken on a  $\text{MgB}_2$  powder sample for  $T \gtrsim T_c$ .

Though  $\text{MgB}_2$  is a two gap superconductor an effective one gap description appears to apply sufficiently close to  $T_c$ [7]. As we concentrate on the effects of thermal fluctuations in the presence of comparatively low magnetic fields we adopt this effective one gap description. Accordingly, the order parameter is assumed to be a single complex scalar. To derive the scaling form of the magnetization in the fluctuation dominated regime we note that the scaling of the magnetic field is in terms of the number of flux quanta per correlation area. Thus, when the thermal fluctuations of

the order parameter dominate the singular part of the free energy per unit volume of a homogeneous system scales as [2, 3, 8, 9, 10, 11, 12, 13]

$$f_s = \frac{Q^\pm k_B T}{\xi_{ab}^2 \xi_c} G^\pm(z) = \frac{Q^\pm k_B T \gamma}{\xi_{ab}^3} G^\pm(z), \quad z = \frac{H_c \xi_{ab}^2}{\Phi_0}. \quad (1)$$

$Q^\pm$  is a universal constant and  $G^\pm(z)$  a universal scaling function of its argument, with  $G^\pm(z=0) = 1$ .  $\gamma = \xi_{ab}/\xi_c$  denotes the anisotropy,  $\xi_{ab}$  the zero-field in-plane correlation length and  $H_c$  the magnetic field applied along the  $c$ -axis. Approaching  $T_c$  the in-plane correlation length diverges as

$$\xi_{ab} = \xi_{ab0}^\pm |t|^{-\nu}, \quad t = T/T_c - 1, \quad \pm = \text{sgn}(t). \quad (2)$$

Supposing that 3D-xy fluctuations dominate the critical exponents are given by [14]

$$\nu \simeq 0.671 \simeq 2/3, \quad \alpha = 2\nu - 3 \simeq -0.013, \quad (3)$$

and there are the universal critical amplitude relations [2, 3, 9, 10, 11, 14]

$$\frac{\xi_{ab0}^-}{\xi_{ab0}^+} = \frac{\xi_{c0}^-}{\xi_{c0}^+} \simeq 2.21, \quad \frac{Q^-}{Q^+} \simeq 11.5, \quad \frac{A^+}{A^-} = 1.07, \quad (4)$$

and

$$A^- \xi_{a0}^- \xi_{b0}^- \xi_{c0}^- \simeq A^- (\xi_{ab0}^-)^2 \xi_{c0}^- = \frac{A^- (\xi_{ab0}^-)^3}{\gamma} = (R^-)^3$$

$$R^- \simeq 0.815, \quad (5)$$

where  $A^\pm$  is the critical amplitude of the specific heat singularity, defined as

$$c = (A^\pm/\alpha) |t|^{-\alpha} + B. \quad (6)$$

Furthermore, in the 3D-xy universality class  $T_c$ ,  $\xi_{c0}^-$  and the critical amplitude of the in-plane penetration depth  $\lambda_{ab0}$  are not independent but related by the universal relation [2, 3, 9, 10, 11, 14],

$$k_B T_c = \frac{\Phi_0^2}{16\pi^3} \frac{\xi_{c0}^-}{\lambda_{ab0}^2} = \frac{\Phi_0^2}{16\pi^3} \frac{\xi_{ab0}^-}{\gamma \lambda_{ab0}^2}. \quad (7)$$

From the singular part of the free energy per unit volume given by (1) we derive for the magnetization per unit volume  $m = M/V = -\partial f_s / \partial H$  the scaling form

$$\frac{m}{T H_c^{1/2}} = -\frac{Q^\pm k_B \xi_{ab}}{\Phi_0^{3/2} \xi_c} F^\pm(z), \quad F^\pm(z) = z^{-1/2} \frac{dG^\pm}{dz},$$

$$z = x^{-1/2\nu} = \frac{(\xi_{ab0}^\pm)^2 |t|^{-2\nu} H_c}{\Phi_0}. \quad (8)$$

In terms of the variable  $x$  this scaling form is similar to Prange's [15] result for Gaussian fluctuations. More generally, the existence of the magnetization at  $T_c$ , of the penetration depth below  $T_c$  and of the magnetic susceptibility above  $T_c$  imply the following asymptotic forms of the scaling function [2, 3, 8, 12, 13]

$$Q^\pm \left. \frac{1}{\sqrt{z}} \frac{dG^\pm}{dz} \right|_{z \rightarrow \infty} = Q^\pm c_\infty^\pm,$$

$$Q^- \left. \frac{dG^-}{dz} \right|_{z \rightarrow 0} = Q^- c_0^- (\ln(z) + c_1),$$

$$Q^+ \left. \frac{1}{z} \frac{dG^+}{dz} \right|_{z \rightarrow 0} = Q^+ c_0^+, \quad (9)$$

with the universal coefficients [2, 8]

$$Q^- c_0^- \simeq -0.7, \quad Q^+ c_0^+ \simeq 0.9, \quad q = Q^\pm c_\infty^\pm \simeq 0.5. \quad (10)$$

The scaling form (8) with the limits (9), together with the critical exponents (3) and the universal relations (4) and (7) are characteristic critical properties of an extreme type II superconductor. They provide the basis to extract from experimental data the doping dependence of the non-universal critical properties, including the transition temperature  $T_c$ , the critical amplitudes of correlation lengths  $\xi_{ab0,c0}^\pm$ , the anisotropy  $\gamma$ , *etc.*, while the universal relations are independent of the doping level.

In practice, however, there are limitations set by the presence of disorder, inhomogeneities and the magnetic field induced finite size effect. Nevertheless, as cuprate superconductors are concerned there is considerable evidence for 3D-xy critical behavior, except for a rounded transition close to  $T_c$  [2, 3, 10, 11, 12, 13, 16, 17, 18, 19, 20, 21, 22, 23, 24]. As disorder is concerned there is the Harris criterion [25], which states that short-range correlated and uncorrelated disorder is irrelevant at the unperturbed critical point, provided that the specific heat exponent  $\alpha$  is negative. Since in the 3D-xy universality class  $\alpha$  is negative (3), disorder is not expected to play an essential role. However, when superconductivity is restricted to homogeneous domains of finite spatial extent  $L_{ab,c}$ , the system is inhomogeneous and the resulting rounded transition uncovers a finite size effect [26, 27] because the correlation lengths  $\xi_{ab,c} = \xi_{ab0,c0}^\pm |t|^{-\nu}$  cannot grow beyond  $L_{ab,c}$ , the respective extent of the homogenous domains. Hence, as long as  $\xi_{ab,c} < L_{ab,c}$  the critical properties of the fictitious homogeneous system can be explored. There is considerable evidence that this scenario accounts for the rounded transition seen in the specific heat [2] and the magnetic penetration depths [28]. In type II superconductors, exposed to a magnetic field  $H_i$ , there is an additional limiting length scale  $L_{H_i} = \sqrt{\Phi_0/(aH_i)}$  with  $a \simeq 3.12$  [29], related to the average distance between vortex lines [3, 29, 30, 31]. Indeed, as the density of vortex lines becomes greater with increasing magnetic field, this cannot continue indefinitely. The limit is roughly set on the proximity of vortex lines by the overlapping of their cores. Due to these limiting lengths the correlation lengths cannot grow beyond [29]

$$\begin{aligned} \xi_i(t_p) &= \xi_{0i}^\pm |t_p|^{-\nu} = L_i, \\ \sqrt{\xi_i(t_p) \xi_j(t_p)} &= \sqrt{\xi_{0i}^\pm \xi_{0j}^\pm} |t_p|^{-\nu} = \sqrt{\Phi_0/(aH_k)} = L_{H_k}, \end{aligned} \quad (11)$$

where  $i \neq j \neq k$ . As the magnetization is concerned the inhomogeneity induced finite size effect is expected to set in close to  $T_c$  where  $\xi_{ab,c}$  approaches  $L_{ab,c}$ , while for a field applied along the c-axis, the magnetic finite size effect dominates when  $L_{H_c} = \sqrt{\Phi_0/(aH_c)} \lesssim L_{ab}$ . Accordingly, sufficiently extended magnetization measurements are not expected to provide estimates for the critical properties of the associated fictitious homogeneous system only, but do have the potential to uncover inhomogeneities giving rise to a finite size effect as well. As a unique size of the homogeneous domains is unlikely, the smallest extent will set the scale where the growth of the respective correlation length starts to deviate from the critical behavior of the homogenous counterpart.

To recognize the implications of the magnetic field induced finite size effect, it is instructive to note that the scaling form of the singular part of the free energy per unit volume, (1), is formally equivalent to an uncharged superfluid, such as  $^4\text{He}$ , constrained to a cylinder of diameter  $L_{H_c} = (\Phi_0/(aH_c))^{1/2}$ . Indeed, the finite size

scaling theory predicts, that in a system confined to a barlike geometry,  $L \cdot L \cdot H$ , with  $H \rightarrow \infty$ , an observable  $O(t, L)$  scales as[26, 27, 32]

$$\frac{O(t, L)}{O(t, \infty)} = f_O(y), \quad y = \xi(t)/L, \quad (12)$$

where  $f(y)$  is the finite size scaling function. As in the confined system a 3D to 1D crossover occurs, there is a rounded transition only. Indeed, because the correlation length  $\xi(t)$  cannot grow beyond  $L$  there is a rounded transition at

$$\begin{aligned} T_p &= T_c \left( 1 - \left( \frac{\xi_0^-}{L} \right)^{1/\nu} \right) : T < T_c. \\ T_p &= T_c \left( 1 + \left( \frac{\xi_0^+}{L} \right)^{1/\nu} \right) : T > T_c. \end{aligned} \quad (13)$$

The resulting rounding of the specific heat singularity and the shift of the smeared peak from  $T_c$  to  $T_p$  is well confirmed in  $^4\text{He}$ [33, 34]. In superconductors the specific heat adopts with (6) and (12) the finite size scaling form

$$c(t, L_{H_c}) = \frac{A^-}{\alpha} |t|^{-\alpha} f_c(t L_{H_c}^{1/\nu}), \quad \nu \simeq 2/3, \quad (14)$$

where

$$f_c(t L_{H_c}^{1/\nu}) = \begin{cases} 1 & : t L_{H_c}^{1/\nu} = 0 \quad : t \leq 0 \\ c_\infty^- (t L_{H_c}^{1/\nu})^\alpha & : t L_{H_c}^{1/\nu} \rightarrow \infty \quad : t < 0 \end{cases} \quad (15)$$

Invoking (13) in the form  $|t_p| = (\xi_{ab0}^-/L_{H_c})^{1/2\nu}$ , the height of the rounded specific heat peak at  $T_p$  vanishes then as

$$\begin{aligned} c(T_p) &= \frac{A^-}{\alpha} |t_p|^{-\alpha} f_c((\xi_{ab0}^-)^{1/\nu}) \\ &= \frac{A^-}{\alpha} \left( \frac{(\xi_{ab0}^-)^2 a}{\Phi_0} \right)^{-\alpha/2\nu} f_c((\xi_{ab0}^-)^{1/\nu}) H_c^{-\alpha/2\nu}, \end{aligned} \quad (16)$$

because  $\alpha < 0$  (3). The resulting shift and reduction of the rounded specific heat peak with increasing magnetic field is in a variety of type II superconductors[29], including  $\text{MgB}_2$ [35, 5], qualitatively well confirmed.

Furthermore, (14) yields with Maxwell's relation

$$\left. \frac{\partial(C/T)}{\partial H_c} \right|_T = \left. \frac{\partial^2 M}{\partial T^2} \right|_{H_c} \quad (17)$$

the scaling form

$$\frac{\partial(c/T)}{\partial H_c} = \frac{\partial^2 m}{\partial T^2} = -\frac{k_B A^\pm}{2\alpha\nu T} H_c^{-1-\alpha/2\nu} |x|^{1-\alpha} \frac{\partial f_c^\pm}{\partial x}. \quad (18)$$

## 2. Experiment, results and analysis

The nearly rectangular shaped  $\text{MgB}_2$  single crystal investigated here was fabricated by high-pressure synthesis described in detail elsewhere[36]. Its calculated volume is  $1.4 \cdot 10^{-5} \text{ cm}^3$  and agrees with susceptibility measurements in the Meissner state with the calculated shape factor 0.81. The magnetic moment was measured by

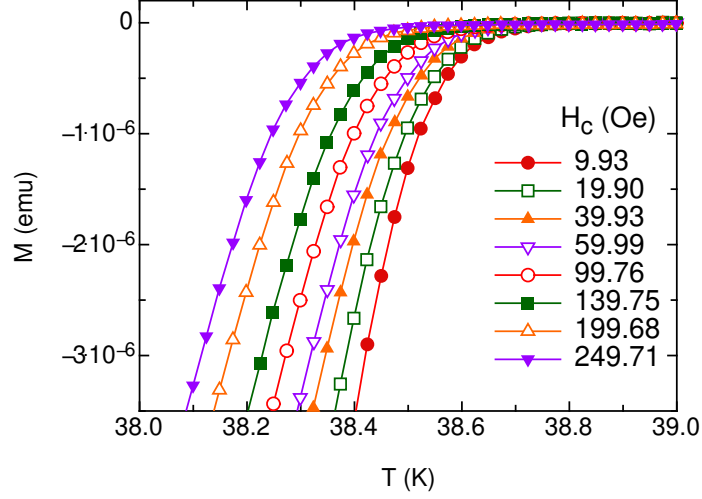


**Figure 1.** Measured magnetic moment of the studied MgB<sub>2</sub> single crystals for different magnetic fields applied along the crystals *c*-axis. The lines are guides to the eye. For clarity not all measured fields are shown.

a commercial Quantum Design DC-SQUID magnetometer MPMS XL allowing to achieve a temperature resolution up to 0.01 K. The installed reciprocating sample option (RSO) allows to measure magnetic moments down to  $10^{-8}$  emu. In our sample this allows to detect the magnetic moment near  $T_c$  down to 25 Oe. The applied magnetic field was oriented along the *c*-axis of the sample. After applying the magnetic field well below  $T_c$  it was kept constant and the magnetic moment of the sample was measured at a stabilized temperature by moving the sample with a frequency of 0.5 Hz through a set of detection coils. The diamagnetic magnetization,  $M = mV$ , was then obtained by subtracting  $M_b = 5 \cdot 10^{-8} H$  emu, the temperature independent paramagnetic and sample holder contributions. Zero-field cooled (ZFC) magnetization curves have been compared to field cooled (FC) data, obtained by cooling to a given temperature in the presence of different fields. Here we concentrate on the reversible regime (see figure 1) close to  $T_c$ . Due to the small volume of the sample its magnetic moment can be reliably detected only below and slightly above  $T_c$ . For this reason we concentrate on the fluctuation effects below and at  $T_c$ .

To estimate  $T_c$  from the magnetization data  $m(T, H_c)$  we invoke the limit  $z \rightarrow \infty$ . Here the scaling form (8) reduces with (9) and (10) to

$$\frac{m}{H_c^{1/2}} = -\frac{k_B q}{\Phi_0^{3/2}} \frac{\xi_{ab}}{\xi_c} T, \quad q = Q^\pm c_\infty^\pm \simeq 0.5. \quad (19)$$

$Q^+ c_\infty^+ = Q^- c_\infty^-$  follows from the fact that  $m/H_c^{1/2}$  adopts at the zero-field transition temperature  $T_c$  a unique value. Here the curves  $m/H_c^{1/2}$  vs.  $T$  taken at different fields  $H_c$  should cross and  $m/H_c^{1/2} \gamma T_c$  adopts the universal value

$$\frac{m \xi_c(T_c)}{H_c^{1/2} T_c \xi_{ab}(T_c)} = -\frac{k_B q}{\Phi_0^{3/2}}. \quad (20)$$

Accordingly, the location of a crossing point in  $m/H_c^{1/2}$  vs.  $T$  provides an estimate for the 3D transition temperature and the factor of proportionality in  $m/T_c$  vs.  $H_c^{1/2}$

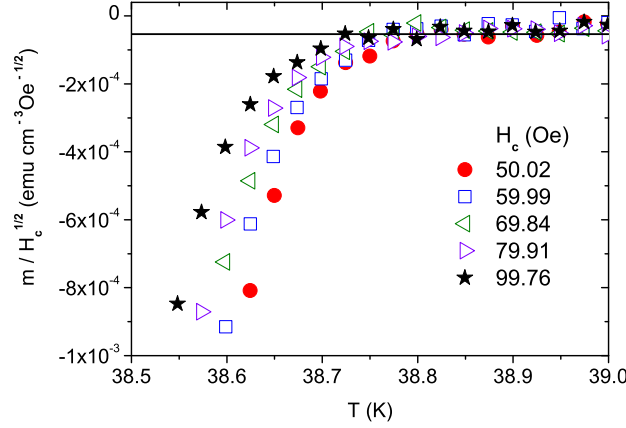


**Figure 2.**  $m/H_c^{1/2}$  vs.  $T$  for a  $\text{MgB}_2$  single crystal with the magnetic field  $H_c$  applied along the  $c$ -axis. The solid line is  $m/(T_c H_c^{1/2}) \approx -1.4 \cdot 10^{-6} (\text{emu cm}^{-3} \text{K}^{-1} \text{Oe}^{-1/2})$  with  $T_c = 38.83$  K.

probes the anisotropy  $\gamma = \xi_{ab}(T_c)/\xi_c(T_c)$ . From Fig. 2 showing  $m/H_c^{1/2}$  vs.  $T$  we derive the estimate  $T_c \simeq 38.83$  K and (20) yields with  $m/(T_c H_c^{1/2}) \approx 1.4 \cdot 10^{-6} (\text{emu cm}^{-3} \text{K}^{-1} \text{Oe}^{-1/2})$  for the anisotropy the value

$$\xi_{ab}(T_c)/\xi_c(T_c) \approx 1.9. \quad (21)$$

In a homogeneous system where the correlation lengths diverge at  $T_c$  as  $\xi_{ab,c} = \xi_{ab0,c0}^\pm |t|^{-\nu}$  with  $\nu \simeq 2/3$ , whereupon  $\xi_{ab}(T_c)/\xi_c(T_c)$  corresponds to the anisotropy  $\gamma = \xi_{ab0}^\pm/\xi_{c0}^\pm$ . In contrast, in an inhomogeneous system, consisting of homogenous domains of spatial extent  $L_{ab,c}$  this ratio probes  $\xi_{ab}(T_c)/\xi_c(T_c) = L_{ab}/L_c$ , because the correlation lengths cannot exceed the homogenous domains. Nevertheless  $\xi_{ab}(T_c)/\xi_c(T_c) \approx 1.9$  is close to  $\gamma \simeq 2$ , the estimate obtained near  $T_c$  with torque magnetometry[37].

According to the scaling form (8) consistency with critical behavior also requires that for low fields the data plotted as  $m/(T H_c^{1/2})$  vs.  $t H_c^{-3/4}$  should collapse near  $t H_c^{-3/4} \rightarrow 0$  on a single curve. Evidence for this collapse emerges from Fig. 3.

Because the limiting magnetic length,  $L_{H_c} = \sqrt{\Phi_0/(a H_c)}$ , decreases with increasing field this scaling behavior does no longer apply at higher fields. Indeed, with increasing field  $L_{H_c} = \sqrt{\Phi_0/(a H_c)}$  approaches  $\xi_{ab}$  and when  $\xi_{ab}(T_p) = L_{H_c}$  the scaling form (19) reduces to

$$\frac{m}{T_p} \simeq -0.5 \frac{k_B}{\Phi_0^{3/2}} \frac{\xi_{ab}(T_p)}{\xi_c(T_p)} H_c^{1/2} = -0.5 \frac{k_B}{\Phi_0 a^{1/2}} \frac{1}{\xi_c(T_p)}, \quad (22)$$

where

$$T_p = T_c \left( 1 - \left( \frac{a H_c (\xi_{ab0}^-)^2}{\Phi_0} \right)^{3/4} \right) = T_c \left( 1 - \left( \frac{\xi_{ab0}^-}{L_{H_c}} \right)^{3/2} \right), \quad (23)$$

in analogy to (13), the expression for  $^4\text{He}$  constrained below  $T_c$  to cylinders of diameter  $L$ . Accordingly, in sufficiently high fields the magnetic field induced finite size effect is predicted to eliminate the characteristic critical field dependence,  $-m/T_c \propto H_c^{1/2}$ , emerging from Fig. 2, because the in-plane correlation length  $\xi_{ab}$  cannot grow beyond



$L_{H_c}$ . A glance to Fig. 4, showing  $-m/T$  vs.  $T$  for various applied magnetic fields in the range from 120 to 300 Oe reveals that this prediction is well confirmed in this field range. Indeed,  $-m/T$  levels off above  $T = T_p$  and the magnitude of  $-m/T_p$  is controlled by  $\xi_c(T_p)$ .

Using Eq.(23),  $T_p(H_c = 299.2 \text{ Oe}) \simeq 38.55 \text{ K}$  and  $T_p(H_c = 119.9 \text{ Oe}) \simeq 38.7 \text{ K}$  we obtain for the critical amplitude of the in-plane correlation length the estimate

$$\xi_{ab0}^- \simeq 52 \text{ \AA}. \quad (24)$$

On this basis the dependence of  $m/(TH_c^{1/2})$  on the scaling variable  $z = (\xi_{ab0}^-)^2 |t|^{-4/3} H_c/\Phi_0$  is then readily calculated. When the magnetic field induced finite size effect scenario holds true, the effective range of the scaling variable is restricted to

$$z \leq 1/a \simeq 0.32, \quad (25)$$

because the correlation length cannot exceed  $\xi_{ab} = L_{H_c}$ . As a consequence (8) reduces for  $z \gtrsim 0.32$  to

$$|t|^{-2/3} \frac{m}{T} = -\frac{k_B}{\Phi_0 \xi_{c0}^-} Q^- \left. \frac{dG^-}{dz} \right|_{z=1/a}. \quad (26)$$

Accordingly, in the plot  $|t|^{-2/3} m/T$  vs.  $z$  the data should collapse and level off for  $z \gtrsim 0.32$ . From Fig. 5, showing this scaling plot, it is seen that this behavior is well confirmed down to  $H_c = 24.86 \text{ Oe}$ , whereupon we obtain for  $L_{ab}$ , the spatial extent of the homogenous domains in the  $ab$ -plane, the lower bound

$$L_{ab} = \left( \frac{\Phi_0}{a H_c} \right)^{1/2} \geq 5.2 \cdot 10^{-5} \text{ cm}, \quad (27)$$

revealing the high quality of the sample.

To check the estimates for the critical amplitudes of the correlation lengths, we invoke, using (8), (9) and (10), the limiting behavior

$$\frac{dm}{d \ln(H_c)} = 0.7 \frac{k_B T}{\Phi_0 \xi_c}, \quad (28)$$

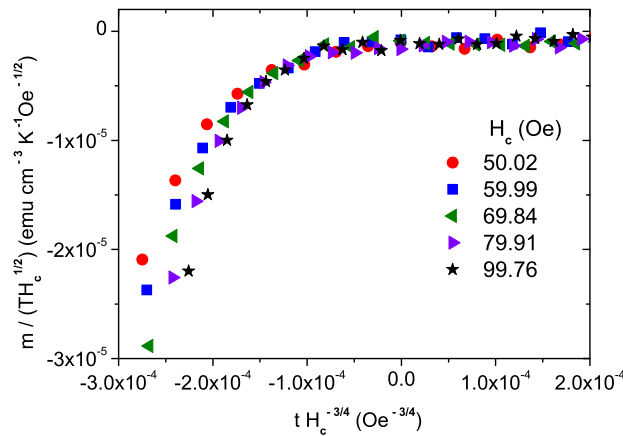


**Figure 3.** Scaling plot  $m/(TH_c^{1/2})$  vs.  $tH_c^{-3/4}$ .

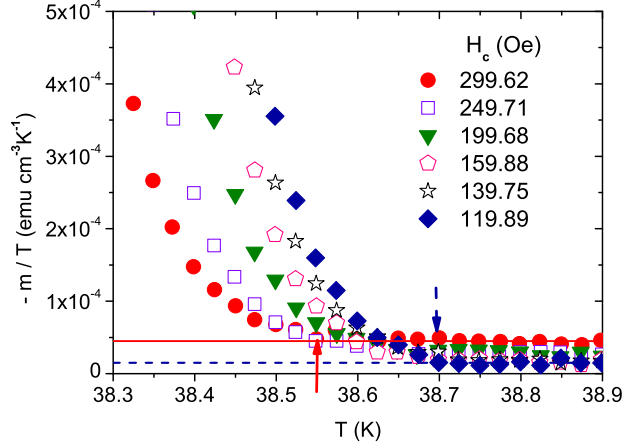


**Figure 4.**  $-m/T$  vs.  $T$  for various applied magnetic fields. The solid line indicates  $-m/T_p = 4.5 \cdot 10^{-5} (\text{emu cm}^{-3} \text{K}^{-1})$  at  $H_c = 299.2$  Oe, where  $T_p \simeq 38.55$  K and the dashed one  $-m/T_p = 1.5 \cdot 10^{-5} (\text{emu cm}^{-3} \text{K}^{-1})$  at  $H_c = 119.9$  Oe, where  $T_p \simeq 38.7$  K. The arrows mark the respective  $T_p$ 's.

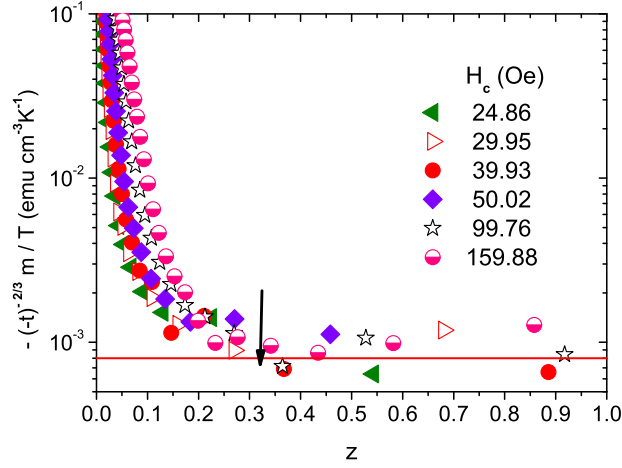


**Figure 5.**  $|t|^{-2/3} m/T$  vs.  $z$  for various fields. The solid line is  $|t|^{-2/3} m/T = 8 \cdot 10^{-4} (\text{emu cm}^{-3} \text{K}^{-1})$  and the arrow marks  $z = 1/a \simeq 0.32$ .

applicable for  $z \rightarrow 0$ . From the plot  $dm/d \ln(H_c)$  vs.  $H_c$  at  $T = 38.7$  K, shown in Fig. 6 and  $dm/d \ln(H_c) = 1.2 \cdot 10^{-3} (\text{emu cm}^{-3} \ln(\text{Oe})^{-1})$  we obtain for the critical amplitude of the  $c$ -axis correlation length the estimate

$$\xi_{c0}^- \simeq 33 \text{ \AA}, \quad (29)$$

in reasonable agreement with  $\xi_{abo}^-/\gamma \simeq 52 \text{ \AA}/1.9 \simeq 27 \text{ \AA}$ . Note that at this temperature and  $\xi_{abo}^- \simeq 52 \text{ \AA}$  the limit  $z \rightarrow 0$  is attained because  $z = 2.74 \cdot 10^{-3} H_c$ , with  $H_c$  in Oe. Together with the universal relation (7),  $\xi_{c0}^- \simeq 33 \text{ \AA}$ , yields for the critical amplitude of the in-plane penetration depth,  $\lambda_{ab0}$ , and the Ginzburg parameter,  $\kappa_{ab0}$ , the estimates

$$\lambda_{ab0} \simeq 7.3 \cdot 10^{-5} \text{ cm}, \quad \kappa_{ab0} = \lambda_{ab0}/\xi_{ab0}^- \simeq 140, \quad (30)$$

which apply very close to  $T_c$ . Unfortunately, the available magnetic penetration depth data does not enter this regime[38, 39].

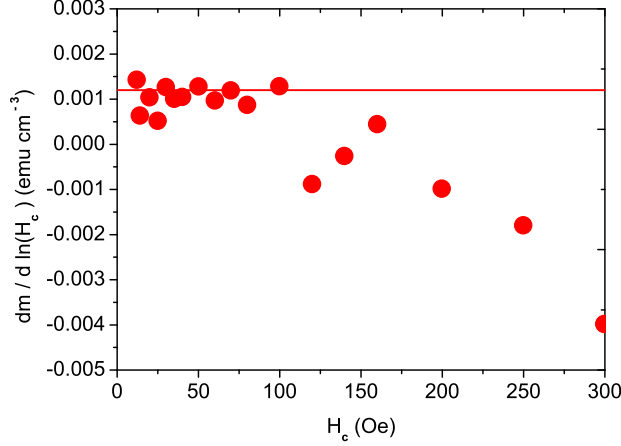


**Figure 6.**  $dm/d \ln(H_c)$  vs.  $H_c$  at  $T = 38.7$  K. The solid line is  $dm/d \ln(H_c) = 1.2 \cdot 10^{-3} (\text{emu cm}^{-3} \ln(\text{Oe})^{-1})$ .

To explore the evidence for an inhomogeneity induced finite size effect, attributable to a system consisting of homogeneous domains of finite extent, we rewrite the scaling form (8) with the aid of (9) in the form

$$\frac{m}{T} = -\frac{k_B}{\Phi_0 \xi_c} Q^- \frac{dG^-}{dz} = -|t|^{2/3} \frac{k_B}{\Phi_0 \xi_{c0}} Q^- \frac{dG^-}{dz} \Big|_{z=H_c L_{ab}^2 / \Phi_0}, \quad (31)$$

because  $\xi_{ab}$  cannot grow beyond  $L_{ab}$ , the extent of the homogeneous domains in the  $ab$ -plane. However, sufficiently close to  $T_c$ ,  $\xi_c$  approaches  $L_c$ , the extent of the homogeneous domains along the  $c$ -axis. Here this scaling form reduces to

$$\begin{aligned} \frac{m}{T} &= -f_0(H_c), \\ f_0(H_c) &= \frac{k_B}{\Phi_0 L_c} Q^- \frac{dG^-}{dz} \Big|_{z=H_c L_{ab}^2 / \Phi_0}. \end{aligned} \quad (32)$$

In Fig. 7 we depicted  $-|t|^{-2/3} m/T$  vs.  $-t$ . Apparently, this limiting behavior is attained roughly below  $-t = -t_{pL_c} = 3 \cdot 10^{-4}$ , where

$$\xi_c(t) = \xi_{c0}^- |t_{pL_c}|^{-2/3} = L_c. \quad (33)$$

With  $\xi_{c0}^- = \xi_{ab0}^- / \gamma \simeq 52 \text{ \AA} / 1.9$  we obtain for  $L_c$ , the  $c$ -axis extent of the homogenous domains, the estimate

$$L_c \approx 6 \cdot 10^{-5} \text{ cm}, \quad (34)$$

which is comparable to the lower bound  $L_{ab} \geq 5.2 \cdot 10^{-5} \text{ cm}$  (27), revealing again the high quality of the sample.

We have seen that the attainable critical regime is limited by both, the magnetic field and inhomogeneity induced finite size effects. The former leads according to (23) in the  $(H, T)$ -plane to the line

$$\begin{aligned} H_{cp}(T) &= \frac{\Phi_0}{a (\xi_{ab0}^-)^2} \left(1 - \frac{T}{T_c}\right)^{4/3} : T < T_c, \\ H_{cp}(T) &= \frac{\Phi_0}{a (\xi_{ab0}^-)^2} \left(\frac{T}{T_c} - 1\right)^{4/3} : T > T_c, \end{aligned} \quad (35)$$

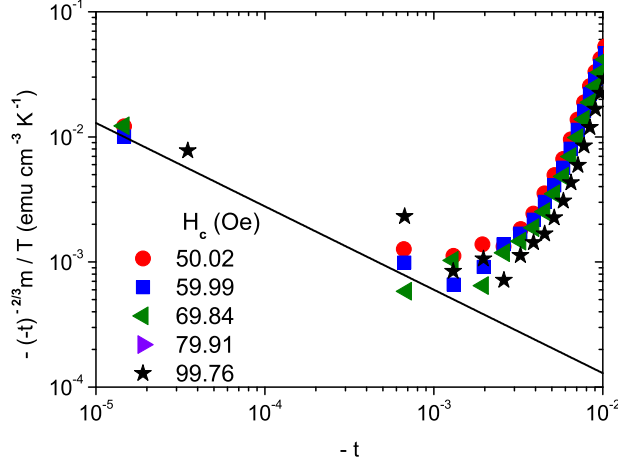


**Figure 7.**  $-|t|^{-2/3} m/T$  vs.  $-t$ . The solid line is  $-|t|^{-2/3} m/T = 6 \cdot 10^{-6} (-t)^{-2/3}$  (emu cm $^{-3}$  K $^{-1}$ ).

depicted in Fig. 8. It is a crossover line because for a fixed temperature, e.g. below  $T_c$ , the limiting length  $L_{H_c} = (\Phi_0 / (aH_c))^{1/2}$  decreases with increasing magnetic field and matches at  $H_{cp}$  the in-plane correlation length  $\xi_{ab}$ . Here and above  $H_{cp}$  superconductivity is then confined to cylinders of diameter  $L_{H_{cp}}$  in the  $ab$ -plane and height  $L_c$  along the  $c$ -axis. Hence in a homogenous system where  $L_c = L_{ab} = \infty$  a 3D to 1D crossover takes place. Even in the presence of inhomogeneities, corresponding to homogeneous domains of extent  $L_{ab,c}$ , this holds true when  $H_c > \Phi_0 / (aL_{ab}^2)$  and  $-t = 1 - T/T_c > (\xi_{c0}^- / L_c)^{3/2}$  because the magnetic field induced finite size effect dominates when  $L_{H_c} < L_{ab}$  and  $\xi_c < L_c$ . Indeed below  $H_c = \Phi_0 / (aL_{ab}^2)$  and

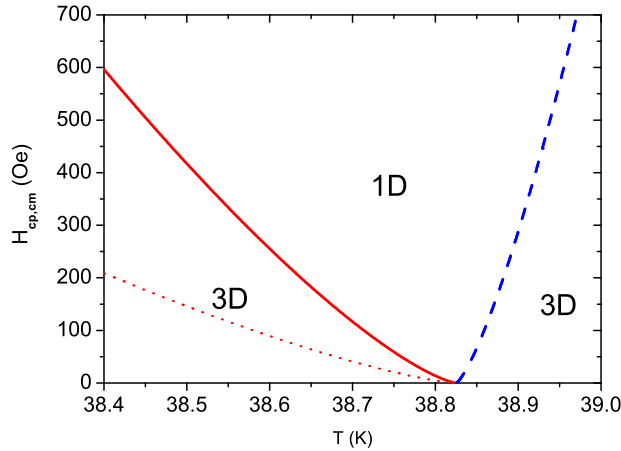


**Figure 8.** Crossover lines  $H_{cp}$  and vortex melting line  $H_{cm}$  vs.  $T$ . The 3D to 1D and the 1D to 3D crossover lines  $H_{cp}$  follows from (35) for  $\xi_{ab0}^- = 52$  Å (24),  $\xi_{ab0}^+ = 52$  Å/2.21  $\simeq$  23.62 Å (4) and  $T_c = 38.83$  K. The solid line applies below  $T_c$  and the dashed line above  $T_c$ . The dotted vortex melting line  $H_{cm}$  follows from (38) and lies at temperatures below the crossover lines  $H_{cp}$ .

$-t = 1 - T/T_c = (\xi_{c0}^-/L_c)^{3/2}$  superconductivity occurs in finite boxes with extent  $L_{ab}^2 L_c$  and above superconductivity is again confined to cylinders and their finite height  $L_c$  is not detected because  $\xi_c < L_c$ . Noting then that in the present case of  $\text{MgB}_2$ ,  $L_{ab} \geq 5.2 \cdot 10^{-5}$  cm (27), the 3D to 1D crossover scenario applies down to fields smaller than 25 Oe, while the finite extent of the homogeneous domains along the  $c$ -axis requires that  $1 - T/T_c \gtrsim 3 \cdot 10^{-4}$  (see Fig. 6), excluding a very narrow temperature range below  $T_c$ .

Finally we show that this scenario is also consistent with the measurements of Lascialfari *et al.*[6] performed on powder samples at  $T \gtrsim T_c$ . The rather large volume of the sample made it possible to explore the critical regime above  $T_c$  as well. To demonstrate the consistency with our analysis we reproduced some data in Fig. 9 in terms of  $m/(TH^{1/2})$  vs.  $T$ . For a powder sample we obtain from (8), (9) and (10) at  $T_c$  the value

$$\frac{m}{T_c H^{1/2}} = -0.5 \frac{k_B \gamma}{\Phi_0^{3/2}} \langle \epsilon(\delta)^3 \rangle, \quad \gamma = \frac{\xi_{ab}}{\xi_c}, \quad (36)$$

where

$$\epsilon(\delta) = \left( \cos(\delta)^2 + \frac{1}{\gamma^2} \sin(\delta)^2 \right)^{1/2}. \quad (37)$$

$\delta$  denotes the random orientation of the applied magnetic field with respect to the  $c$ -axis and  $\langle \epsilon(\delta)^3 \rangle$  is the corresponding average. For  $\gamma = 1.9$  we obtain  $\langle \epsilon(\delta)^3 \rangle \simeq 0.541$  and with that  $m/(T_c H^{1/2}) \simeq -1.44 \cdot 10^{-6}$  (emu cm $^{-3}$  K $^{-1}$  Oe $^{-1/2}$ ). Perfect agreement with our analysis emerges from Fig. 9 for  $T_c \simeq 39.17$  K, consistent with the observation of Lascialfari *et al.*[6] that in this sample  $T_c$  is near 39.1 K. To explore the occurrence of the vortex melting transition and the 3D to 1D crossover we displayed in Fig. 10 the data of Lascialfari *et al.*[6] according to the scaling form (18). The minimum at  $t_p H^{-3/4} \simeq -3.4 \cdot 10^{-3}$  Oe $^{-3/4}$  locates the 3D to 1D crossover line, while the peak at  $t_m H^{-3/4} \simeq -7.5 \cdot 10^{-3}$  Oe $^{-3/4}$  signals the vortex melting transition. For the ratio of

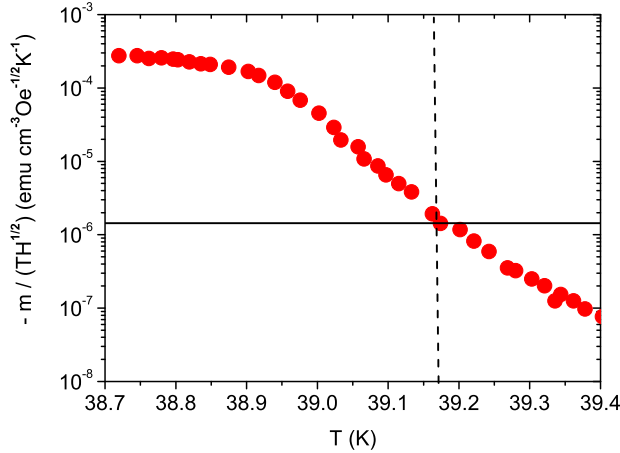


**Figure 9.**  $m/(TH^{1/2})$  vs.  $T$  at  $H = 1$  Oe for the  $\text{MgB}_2$  powder sample of Lascialfari *et al.*[6]. The horizontal line is  $m/(T_c H^{1/2}) \simeq -1.44 \cdot 10^{-6}$  (emu cm $^{-3}$  K $^{-1}$  Oe $^{-1/2}$ ) and the vertical one marks  $T_c \simeq 39.17$  K.

the universal values of the scaling variable  $z$  at the melting and the 1D to 3D crossover line we obtain the estimate

$$z_m/z_p = (t_p(H)/t_m(H))^{4/3} \simeq 0.35, \quad (38)$$

in reasonable agreement with  $z_m/z_p \simeq 0.25$ , the value emerging from the specific heat data of Roulin *et al.*[23] for  $\text{YBa}_2\text{Cu}_3\text{O}_{6.97}$ . The resulting vortex melting line is included in Fig. 8.

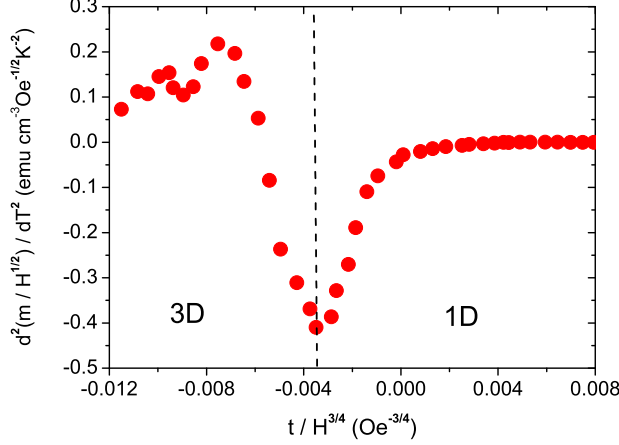


**Figure 10.**  $d^2(m/H^{1/2})/dT^2$  vs.  $t/H^{3/4}$  for  $H = 1$  Oe derived from the data of Lascialfari *et al.*[6]. The minimum at  $t_p H^{-3/4} \simeq -3.4 \cdot 10^{-3} \text{ Oe}^{-3/4}$  locates the 3D to 1D crossover line, while the peak at  $t_m H^{-3/4} \simeq -7.5 \cdot 10^{-3} \text{ Oe}^{-3/4}$  signals the vortex melting transition.

At higher fields and fixed temperature, however, a crossover from  $m/T \propto H$  to  $m/T = \text{const}$  is expected to occur. Indeed, approaching the limit  $z \rightarrow 0$ , the scaling form

$$\frac{m}{T} = -0.9 \frac{k_B \xi_{ab}^2}{\Phi_0^2 \xi_c} \langle \epsilon(\delta)^2 \rangle H, \quad (39)$$

applies according to (8), (9) and (10). As the scaling variable  $z$  increases with rising magnetic field it approaches the value  $z = 1/a$  where the magnetic field induced finite size effect sets in. Here the scaling expression (8) applies in the form

$$\frac{m}{T} = -\frac{k_B}{\Phi_0 \xi_c} \langle \epsilon(\delta) \rangle Q^+ \left. \frac{dG^+}{dz} \right|_{z=1/a}, \quad (40)$$

for  $z \geq 1/a$ , where

$$z = \frac{H \xi_{ab}^2}{\Phi_0} \epsilon(\delta) \quad (41)$$

From Fig. 11, showing  $m/T$  vs.  $H$  at  $T = 39.3$  K for the  $\text{MgB}_2$  powder sample of Lascialfari *et al.*[6], it is seen that this behavior, including the saturation due to the magnetic field induced finite size effect, is well confirmed. Therefore, in analogy to the situation below  $T_c$ , there is a magnetic field induced finite size effect above  $T_c$  as well. However, there is no long range order in this regime so that uncondensed pairs are forced to confine above  $H_{cp}(T)$  (see Fig. 8) in cylinders of diameter  $L_{H_{cp}}$ .

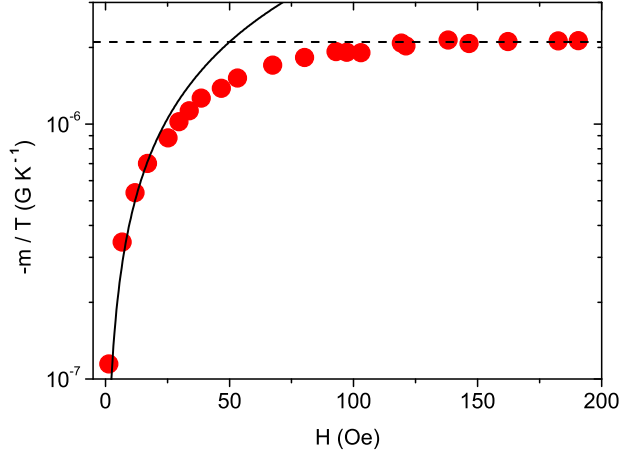


**Figure 11.**  $m/T$  vs.  $H$  at  $T = 39.3$  K for the  $\text{MgB}_2$  powder sample of Lascialfari *et al.*[6]. The solid line is  $m/T = -4.2 \cdot 10^{-8} H$  ( $\text{GK}^{-1}$ ) and the dashed one  $m/T = -2.1 \cdot 10^{-6} (\text{GK}^{-1})$ , marking the saturation due to the magnetic field induced finite size effect.

### 3. Summary

To summarize, our scaling analysis of reversible magnetization data of a  $\text{MgB}_2$  single crystal with the magnetic field applied along the  $c$ -axis provided considerable evidence that even in this type II superconductor the 3D-xy critical regime is experimentally accessible, provided that the sample is sufficiently homogeneous. The high quality of our sample allowed to explore the occurrence of the magnetic field induced finite size effect down to rather low magnetic fields where 3D-xy fluctuations still dominate. In this regime we were able to provide rather unambiguous evidence for this finite size effect. It implies that in type II superconductors, such as  $\text{MgB}_2$ , exposed to a magnetic field superconductivity is confined to cylinders. Their diameter is given by the limiting magnetic length  $L_{H_i} = (\Phi_0 / (aH_i))^{1/2}$ , whereupon for a magnetic field applied parallel to the  $i$ -axis, there is the line  $H_{pi}(T) = (\Phi_0 / (a\xi_{j0}^-\xi_{k0}^-)) (1 - T/T_c)^{4/3}$  with  $i \neq j \neq k$ , where below  $T_c$  a 3D to 1D crossover takes place.  $\xi_{i0,j0,k0}^-$  denote the critical amplitudes of the correlation length below  $T_c$  along the respective axis. Accordingly, there is below  $T_c$  no continuous phase transition in the  $(H, T)$  -plane along the  $H_{c2}$ -lines as predicted by the mean-field treatment. Our scaling analysis of the magnetization data of Lascialfari *et al.*[6] also confirmed that the magnetic field induced finite size effect is not restricted to the superconducting phase ( $T < T_c$ ). Indeed, above  $T_c$  there is the line  $H_{pi}(T) = (\Phi_0 / (a\xi_{j0}^+\xi_{k0}^+)) (T/T_c - 1)^{4/3}$  where the 3D to 1D crossover occurs and uncondensed pairs are forced to confine in cylinders. Furthermore, we have shown that the scaling analysis of magnetization data also opens a door onto the ascertainment of the homogeneity of the sample in terms of the finite size effect arising from the limited extent of the homogenous domains.

### 4. Acknowledgments

The authors are grateful to J. Roos for the help to prepare the manuscript and useful comments. This work was supported by the Swiss National Science Foundation and in part by the NCCR program MaNEP.

## 5. References

- [1] Nagamatsu J, Nakagawa N, Maranaka T, Zenitani Y and Akimitsu J 2001 *Nature (London)* **410** 63
- [2] Schneider T and Singer J M 2000 *Phase Transition Approach To High Temperature Superconductivity* (Imperial College Press, London)
- [3] Schneider T 2004 *The Physics of Superconductors* edited by K. Bennemann and J. B. Ketterson (Springer, Berlin) p. 111
- [4] Kang W N *et al* 2002 *J. Korean Phys. Soc.* **40** 949
- [5] Park Tuson, Salamon M B, Jung C U, Park Min-Seok, Kim Kyunghhee and Lee Sung-Ik 2002 *Phys. Rev. B* **66** 134515
- [6] Lascialfari A, Mishonov T, Rigamonti A, Tedesco P and Varlamov A 2002 *Phys. Rev. B* **65** 180501(R)
- [7] Dao V H and Zhitomirski M E 2005 *Eur. Phys. J. B* **44** 183
- [8] Hofer J, Schneider T, Singer J M, Willemin M, Keller H, Sasagawa T, Kishio K, Conder K and Karpinski J 2000 *Rev. B* **62** 631
- [9] Fisher D S, Fisher M P A and Huse D A 1991 *Phys. Rev. B* **43** 130
- [10] Schneider T and Ariosa D 1992 *Z. Phys. B* **89** 267
- [11] Schneider T and Keller H 1993 *Int. J. Mod. Phys. B* **8** 487
- [12] Schneider T, Hofer J, Willemin M, Singer J M and Keller H 1998 *Eur. Phys. J. B* **3** 413
- [13] Hofer J, Schneider T, Singer J M, Willemin M, Keller H, Rossel C and Karpinski J 1999 *Phys. Rev. B* **60** 1332
- [14] Pelissetto A and Vicari E 2002 *Physics Reports* **368** 549
- [15] Prange R E 1970 *Phys. Rev. B* **1** 2349
- [16] Hubbard M A, Salamon B and Veal B W 1996 *Physica C* **259** 309
- [17] Babic D, Cooper J R, Hodby J W and Changkang Chen 1999 *Phys. Rev. B* **60** 698
- [18] Overend N, Howson M A and Lawrie I D 1994 *Phys. Rev. Lett.* **72** 3238
- [19] Kamal S, Bonn D A, Goldenfeld N, Hirschfeld P J, Liang R and Hardy W N 1994 *Phys. Rev. Lett.* **73** 1845
- [20] Jaccard Y, Schneider T, Looquet J P, Williams E J, Martinoli P and Fischer Ø 1996 *Europhys. Lett.* **34** 281
- [21] Kamal S, Liang R, Hosseini A, Bonn D A and Hardy W N 1998 *Phys. Rev. B* **58** R8933
- [22] Pasler V, Schweiss P, Meingast Ch, Obst B, Wühl H, Rykov A I and Tajima S 1998 *Phys. Rev. Lett.* **81** 1094
- [23] Roulin M, Junod A and Walker E 1998 *Physica C* **296** 137
- [24] Schneider T 2007 *Phys. Rev. B* **75** 174517
- [25] Harris A B 1974 *J. Phys. C* **7** 1671
- [26] Cardy J L ed. 1988 *Finite-Size Scaling* North Holland Amsterdam
- [27] Privman V 1990 *Finite Size Scaling and Numerical Simulations of Statistical Systems*, World Scientific NJ
- [28] Schneider T and Di Castro D 2004 *Phys. Rev. B* **69** 024502
- [29] Schneider T *Journal of Superconductivity* 2004 **17** 41
- [30] Haussmann R 1999 *Phys. Rev. B* **60** 12373
- [31] Lortz R, Meingast C, Rykov A I and Tajima S 2003 *Phys. Rev. Lett.* **91** 207001
- [32] Nho K and Manousakis E 2001 *Phys. Rev. B* **64** 144513
- [33] Coleman M and Lipa J A 1995 *Phys. Rev. Lett.* **74** 286
- [34] Gasparini F M, Kimball M O and Mooney K P 2001 *J. Phys.: Condens. Matter* **13** 4871
- [35] Lyard L *et al.* 2002 *Phys. Rev B* **66** 180502(R)
- [36] Karpinski J *et al.* 2003 *Supercond. Sci. Technol.* **16** 221
- [37] Angst M, Puzniak R, Wisniewski A, Jun J, Kazakov S M, Karpinski J, Roos J and Keller H 2002 *Phys. Rev. Lett.* **88** 167004
- [38] Panagopoulos C, Rainford B D, Xiang T, Scott C A, Kambara M and Inoue I H, 2001 *Phys. Rev. B* **64** 094514
- [39] Di Castro D, Khasanov R, Grimaldi C, Karpinski J, Kazakov S M, Brütsch R and Keller H 2005 *Phys. Rev. B* **72** 094504